

# Spin-Polarized Tunnelling, Discrete Energy Levels, and Spin-Relaxation in Nanometer-Scale Aluminum Grains

Y. G. Wei, C. E. Malec, D. Davidović  
*Georgia Institute of Technology, Atlanta, GA 30332*  
(Dated: June 27, 2019)

We describe measurements of spin-polarized tunnelling via discrete energy levels of single Aluminum grains. In high resistance samples ( $\sim G\Omega$ ), spin-polarized current is carried only via the ground state and the low-lying excited states. In two samples, the spin-relaxation rate  $T_1^{-1}$  for some of the low-lying excited states is comparable to the electron tunnelling rate:  $T_1^{-1} \approx 1.5 \cdot 10^6 s^{-1}$  and  $10^7 s^{-1}$ . So, the spin of an electron confined in a metallic grain is highly stable, making it a viable candidate for quantum information studies. The ratio of  $T_1^{-1}$  to the electron-phonon relaxation rate is in quantitative agreement with the Elliot-Yafet scaling, an evidence that spin-relaxation in Al grains is driven by the spin-orbit interaction.

Electron tunnelling through single nanometer scale metallic grains at low temperatures can display a discrete energy level spectrum. [1] Tunnelling spectroscopy of the energy spectra have led to numerous discoveries, including Fermi-Liquid coupling constants between quasiparticles, [2] spin-orbit interactions, [3, 4] and superconducting correlations in zero-dimensional systems. [5] Some information regarding the spin of an electron occupying a discrete level can be obtained using spin-unpolarized tunnelling, such as spin-multiplicity and electron g-factors. [1]

In this letter we report on spin-polarized tunnelling via discrete energy levels of single aluminum grains. Spin-polarized electron transport permits studies of spin relaxation and spin dephasing. [6, 7] We find that some electron spin-relaxation times in Al grains are exceptionally long, on the order of  $\mu s$ . This finding is analogous to the discovery of  $\mu s$  long spin-relaxation times in semiconducting quantum dots, [8, 9] which is the basis of a proposal to use electron spins in quantum dots as quantum bits. [10] Our findings demonstrate that the electron spin in a metallic grain is also a viable candidate for quantum information research.

Spin-polarized transport via metallic grains has generated recently significant theoretical interest. [11, 12, 13, 14, 15] In addition, there is a major effort to study nano-spintronics using carbon-nanotubes; see Ref. [16] and references therein. Spin-coherent electron tunnelling via nanometer scale normal metallic grains has been confirmed in arrays [17] and in single grains. [18] However, the electron spin-relaxation time  $T_1$  in a metallic grain has not been reported yet.

Our samples are prepared by electron beam lithography and shadow evaporation, similar to the technique described previously. [3] First we define a resist bridge placed 250 nm above the Si wafer; this bridge acts as a mask. Next (Fig. 1-A), we deposit 11 nm permalloy ( $\text{Py} = \text{Ni}_{0.8}\text{Fe}_{0.2}$ ) onto oxidized silicon substrate at  $4 \cdot 10^{-7}$  Torr base pressure, measured near the gate valve, along the direction indicated by the arrow. Then we rotate the sample by 36 degrees without breaking the vacuum and

deposit 1.2 nm of  $\text{Al}_2\text{O}_3$  by reactive evaporation of Al, [3] at a rate of 0.35 nm/s, at an oxygen pressure of  $2.5 \cdot 10^{-5}$  Torr. Now, oxygen flow is shut down. When pressure decreases to the  $10^{-7}$  Torr range, we deposit a 0.6 nm thick film of Al, as shown in Fig. 1-B. Al forms isolated grains with a typical diameter of 5 nm. The grains are displayed by the scanning electron microscope (SEM) image in Fig. 1-D. Finally we deposit another 1.2 nm layer of  $\text{Al}_2\text{O}_3$  by the reactive evaporation and top it off by an 11 nm thick film of Py (Fig. 1-C).

We make many samples on the same silicon wafer, and vary the overlap from 0 to 50 nm and select the devices with the highest resistance, as they have the smallest overlap. Figs. 1-E and F show SEM images of a typical device.

Transport properties of the samples at low temperatures were measured using an Ithaco current amplifier. The samples were cooled down to  $\approx 0.035K$  base temperature. The sample leads were cryogenically filtered to reduce the electron temperature down to  $\approx 0.1K$ .

The majority of samples ( $>80\%$ ) exhibit Coulomb Blockade at low temperature. About 150 samples were measured at  $4.2K$  and 16 samples at  $0.035K$ . In this paper we describe two samples. The I-V curve of two samples are shown in Fig. 1-G and H. The tunnelling current increases in discrete steps as a function of bias voltage, corresponding to discrete electron-in-a-box energy levels of the grain.

By following standard analysis techniques, [19] we determine the junction capacitances  $C_L$  and  $C_R$  and the tunnelling rates  $\Gamma_{L,R}^i$  between the excited states  $i$  and leads  $L$  and  $R$ . Our samples have highly asymmetric resistances, which is expected in metallic grains. The rate limiting tunnelling takes place at the higher resistance tunnelling junction, which connects the grain to lead  $L$  in sample 1. For beginning, in further discussions we select the sign of the bias voltage so that the first tunnelling step is rate limiting. The Coulomb Blockade in this case has a weak effect on the current through energy levels, and the current steps in equilibrium transport would be  $2|e|\Gamma_L^i$ .

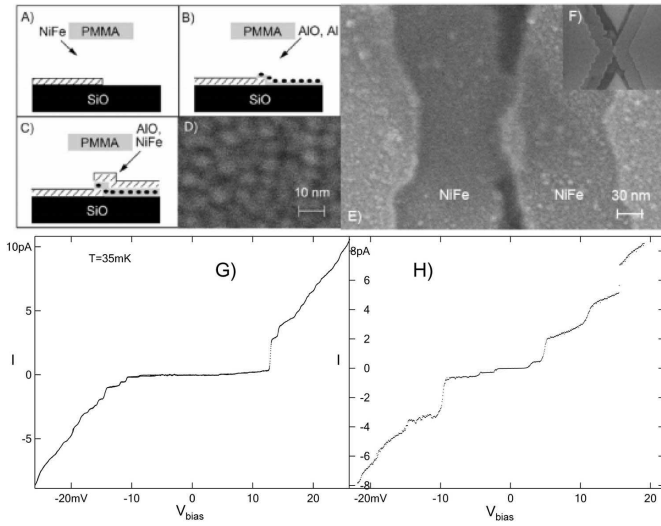


FIG. 1: A, B, C: Sample fabrication steps. D. Image of Al grains. E, F: Image of a typical sample. G, H: I-V curves at the base temperature.

In sample 1, the average electron-in-a-box level spacing caused by electron geometric confinement is  $\delta \approx 0.8\text{meV}$ , which corresponds to diameter of  $D \approx 6\text{nm}$  assuming a spherical Al grain. The average current step is  $\bar{I} \approx 0.47\text{pA}$ , which corresponds to the average tunnelling-in rate of  $\bar{\Gamma}_L = \bar{I}/2|e| \approx 1.5 \cdot 10^6\text{s}^{-1}$ ; the tunnelling-out rates are much larger. Similarly, in sample 2,  $\delta \approx 2.7\text{meV}$ ,  $D \approx 4\text{nm}$ , and  $\bar{\Gamma}_R \approx 9.6 \cdot 10^6\text{s}^{-1}$ .

As shown by Fig. 2, the energy levels exhibit Zeeman splitting as a function of an applied magnetic field. In sample 1, the I-V curve probes the same energy spectrum at negative and positive bias voltage. This is evident from the equivalence of the magnetic field dependences at negative and positive bias. The lowest tunnelling threshold is two fold degenerate at zero magnetic field, showing that  $N_0$ , the number of electrons on the grain before tunnelling in, is even.

In sample 1, the first two current steps split corresponding to g-factors:  $g = 1.83 \pm 0.05$  and  $1.95 \pm 0.05$ . Slight reduction of the g-factors from 2 indicates spin-orbit interaction in Al. [1] The avoided level crossings clearly are resolved in Fig. 2. In the regime where g factors are slightly reduced, the spin-orbit scattering rate ( $\tau_{SO}^{-1}$ ) can be obtained from the avoided crossing energies  $\Delta_{SO} \approx 0.1\text{meV}$ . [20] Theory predicts that  $\tau_{SO} \approx \hbar\delta/\pi\Delta_{SO}^2$ , [20] within a factor of two. Thus, we obtain  $\tau_{SO}^{-1} \approx 5.5 \cdot 10^{10}\text{s}^{-1}$ . By the Elliot-Yafet relation, [21]  $\tau_{SO}^{-1}$  is related to the elastic scattering rate  $\tau_e^{-1}$ :  $\tau_{SO}^{-1} = \alpha\tau_e^{-1}$ . Assuming ballistic grain,  $\tau_e^{-1} \approx v_F/D = 3.4 \cdot 10^{14}\text{sec}^{-1}$ . We obtain  $\alpha \approx 1.6 \cdot 10^{-4}$ , in excellent agreement with  $\alpha \approx 10^{-4}$  in Al thin films. [22]

Now we discuss spin-polarized tunnelling. In the magnetic field range of  $\pm 50\text{mT}$ , 90% of the samples do not display any tunnelling magnetoresistance (TMR). By

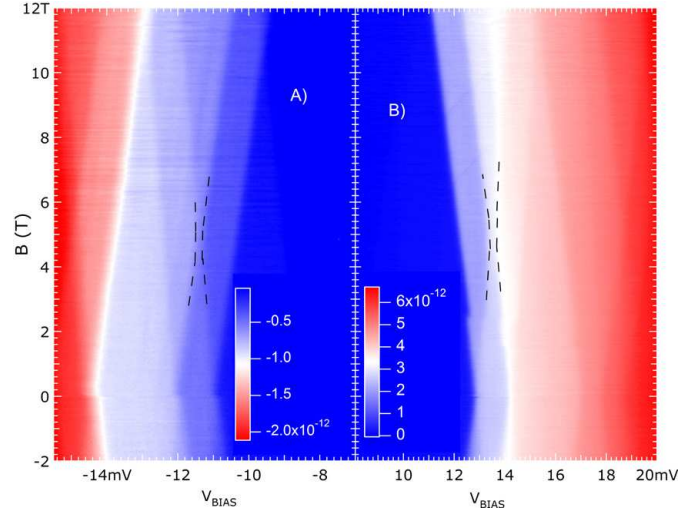


FIG. 2: A, B: Current (color) versus bias voltage and the applied magnetic field in sample 1 at the base temperature.

contrast, we tested about 10 tunnelling junctions without the embedded grains and with similar resistance (empty junctions) at 4.2 K. All of the empty junctions in this field range exhibit a significant TMR, comparable to 10%. Approximately one half of the empty junctions display a straightforward spin-valve effect. So, the absence of TMR for electron tunnelling via grains shows that the spin-dephasing rate  $T_2^{-1}$  in the grains must be typically much larger than the tunnelling rate.

Nevertheless, approximately 10% of the samples with embedded grains display significant TMR, so in these samples  $T_2^{-1}$  must be smaller than or comparable to the tunnelling rate. The TMR in these samples usually does not display a straightforward spin-valve effect. In a future publication, we will show that there are spin-dependent interactions inside the grain that can induce a complicated TMR even if the magnetic transitions in the drain and source leads are straightforward and sharp. These interactions include the Zeeman effect in the stray field and the hyperfine interaction with the nuclei.

$T_2$  variation among different samples suggests that the dephasing is caused by defects. One possibility could be paramagnetic impurities from the Py layer, since paramagnetic impurities are common sources of dephasing. [23] These defects would be located on the grain surface, since bulk Al does not support paramagnetic impurities. Given the small number of atoms on the surface ( $\sim 1000$ ), we could occasionally obtain a sample free of impurities, and a  $T_2$  longer than the tunnelling time.

We select two samples that display a straightforward spin-valve effect in TMR, which is displayed in Figs. 3. Fig. 3-A is the TMR of sample 1 at a bias voltage corresponding to the second current plateau. TMR is barely resolved in this case, since the current changes by only about 40fA. By comparison, Figs. 3-B and C display

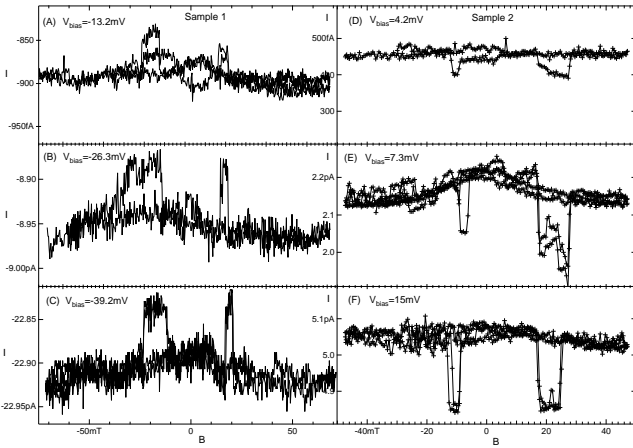


FIG. 3: A-F: Spin-valve effect in current versus applied magnetic field in two samples at the base temperature. The current magnitude is reduced in the antiparallel state.

TMR at bias voltage where the number of electron-in-a-box levels energetically available for tunnelling-in are approximately 19 and 48, respectively. To facilitate comparisons, the current intervals on the vertical axes in Figs. 3 A-C and D-F have equal lengths.

The key observation in this letter is that  $\Delta I = I_{\uparrow\uparrow} - I_{\uparrow\downarrow}$  is nearly constant with current above a certain current. There is hardly any increase in  $\Delta I$  between Figs. 3 B and C and between Figs. 3 E and F. This behavior is shown in more detail Fig. 4-A and B, which displays  $\Delta I$  versus bias voltage.  $\Delta I$  versus negative bias voltage in sample 1 is fully saturated at the third current plateau; at the second current plateau,  $\Delta I$  is already at one half of the saturation value. Similarly, in sample 2  $\Delta I$  reaches saturation at the second current plateau. Our samples should be contrasted with ordinary ferromagnetic tunnelling junctions, where  $\Delta I$  is proportional to the current.

To explain  $I_{\uparrow\uparrow} - I_{\uparrow\downarrow} = \text{const}$ , consider tunnelling via the grain at a large bias voltage such that the number of electron-in-a-box levels energetically available for tunnelling-in is large. Since we assume that tunnelling-in is the rate limiting step, which is the case in our samples at bias voltages where we study TMR, the grain spends most of the time in the states with  $N_0$  electrons.

The spin-conserving energy-relaxation in Al grains takes place by phonon emission with the relaxation rate [2]

$$\frac{1}{\tau_{e-ph}(\omega)} = \left( \frac{2}{3} E_F \right)^2 \frac{\omega^3 \tau_e \delta}{2 \rho \hbar^5 v_s^5}, \quad (1)$$

where  $E_F = 11.7\text{eV}$  is the Fermi energy,  $\omega$  is the energy difference between the initial and the final state,  $\rho = 2.7\text{g/cm}^3$  is the ion-mass density, and  $v_s = 6420\text{m/s}$  is the sound velocity. We obtain  $\tau_{e-ph}^{-1}(\delta) \approx 1.6 \cdot 10^9 \text{s}^{-1}$  and  $4.1 \cdot 10^{10} \text{s}^{-1}$  in samples 1 and 2, respectively. Sample

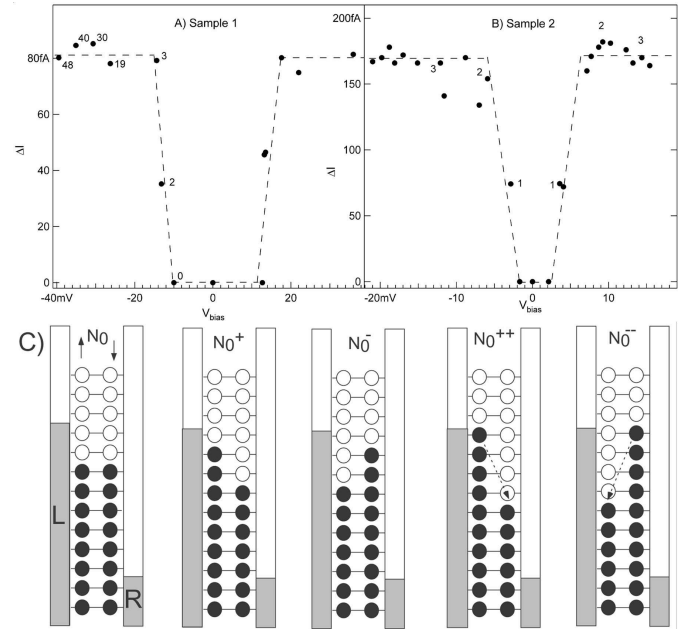


FIG. 4: A and B:  $\Delta I = |I_{\uparrow\uparrow} - I_{\uparrow\downarrow}|$  versus bias voltage in samples 1 and 2, respectively, at the base temperature. The numbers near the circles indicate how many doubly degenerate electron-in-a-box levels are available for tunnelling in. C: Possible spin-polarized electron configurations caused by electron tunnelling in and out, before an electron tunnels in, at the second current plateau, for  $N_0$  even.

2 has significantly larger relaxation rate because of the larger level spacing.

By comparison, the tunnelling rates in our samples are  $\sim 10^6 \text{s}^{-1}$ . If the grain is excited by electron tunnelling in and out, it will instantly relax to the lowest energy state accessible by spin-conserving transitions. But the rate of spin-flip transitions could be significantly smaller than  $\tau_{e-ph}^{-1}$ . In this case the ground state would not always be accessible by energy relaxation. The grain could remain in an excited, spin-polarized state, as sketched in Fig. 4-C.

These spin-polarized excited states are responsible for spin accumulation in the antiparallel magnetic configuration of the leads. If the relaxation rates for the spin-flip transitions are much smaller than the tunnelling rate, then various spin-polarized states would have similar probabilities, except that probabilities of the excitations with spin up would be enhanced by  $1 + P$  and probabilities of the excitations with spin down would be suppressed by  $1 - P$ , where  $P$  is the spin-polarization in the leads. In this regime we find  $I_{\uparrow\uparrow} - I_{\uparrow\downarrow}$  to be proportional to the current, similar to the usual ferromagnetic tunnelling junctions.

But we expect that the spin-flip rate  $T_1^{-1}(\omega)$  increases rapidly with energy difference  $\omega$  between the initial and the final state. If  $T_1^{-1}(\omega)$  exceeds the tunnelling rate above some  $\omega$ , then those excitations with energy  $> \omega$

will occur with a reduced probability in the ensemble of states generated by tunnelling in and out. Thus  $\Delta I$  is limited by tunnelling via the ground state and those low lying spin-polarized states where  $T_1^{-1}(\omega) < \Gamma_L$ .  $\Delta I$  versus bias voltage approaches saturation approximately when  $T_1^{-1}(\omega) = \Gamma_L$ , where  $\omega$  is the highest excitation energy in the ensemble of spin-polarized states generated by tunnelling in and out:  $\omega \approx \delta \frac{I}{|e|\Gamma_L}$ . This is how we can determine the spin-relaxation time  $T_1(\omega)$  at one energy  $\omega$  in a given sample.

A precise mathematical formulation of electron transport via discrete energy levels with nonequilibrium effects and spin relaxation is beyond the scope of this letter. We have performed this analysis in detail, by extending the methods obtained in Ref. [19]. Our analysis shows that  $\Delta I$  is proportional to a weighted sum of the probabilities of various spin-polarized states. The probabilities of the spin-polarized states where  $T_1^{-1}(\omega) \gg \Gamma_L$  are suppressed by factor of  $T_1(\omega)\Gamma_L$ ; the suppression leads to the saturation in  $\Delta I$  versus bias voltage.

In sample 1 where  $N_0$  is even,  $\Delta I$  reaches 50% of the saturation value at the second current plateau, and  $\Delta I$  is nearly fully saturated at the third current plateau. At the second current plateau, the spin-relaxation rate of the highest energy excited state generated by tunnelling must be close to the tunnelling rate. The grain spends most of the time among five configurations:  $N_0$ ,  $N_0^+$ ,  $N_0^-$ ,  $N_0^{++}$ , and  $N_0^{--}$ , as shown in Fig. 4-C. The highest energy spin-polarized states are  $N_0^{++}$  and  $N_0^{--}$ . They are at energy  $3\delta$  above the ground state. Thus,  $T_1^{-1}(3\delta) \approx \Gamma_L = 1.5 \cdot 10^6 s^{-1}$ . In sample 2, similar analysis leads to  $T_1^{-1}(2\delta) \approx 10^7 s^{-1}$ .

Now we discuss the origin of spin relaxation and its rapid enhancement with the energy difference. Note that the rate of spin-conserving transitions in Eq. 1 increases as  $\omega^3$ . We hypothesize that the spin-flip and the electron-phonon transition rates scale by the Elliot-Yafet relation:  $T_1^{-1}(\omega) = \alpha' \tau_{e-ph}^{-1}(\omega)$ . This scaling would explain the observed rapid increase in spin-relaxation rate with  $\omega$ . In metallic films, it is well established that the Elliot-Yafet scaling applies for both elastic and inelastic scattering processes, with  $\alpha \approx \alpha'$ . [22]

In sample 1, Eq. 1 leads to  $\tau_{e-ph}^{-1}(3\delta) \approx 4 \cdot 10^{10} s^{-1}$ . Since  $T_1^{-1}(3\delta) \approx 1.5 \cdot 10^6 s^{-1}$ , we obtain  $\alpha' \approx 0.4 \cdot 10^{-4}$ . Similarly, in sample 2,  $\tau_{e-ph}^{-1}(2\delta) \approx 3.3 \cdot 10^{11} s^{-1}$  and we obtain  $\alpha' \approx 0.3 \cdot 10^{-4}$ .  $\alpha'$  agrees with  $\alpha \approx 1.5 \cdot 10^{-4}$  obtained earlier, within an order of magnitude. So the ratio of  $\tau_{e-ph}$  and  $T_1$  is in agreement with the Elliot-Yafet scaling. This is an evidence that the spin-flip transitions in Al grains are driven by the spin-orbit interaction. By this relaxation mechanism, the spin of an electron on the grain is coupled to the phonon continuum via the spin-orbit interaction. An electron in an excited spin-polarized state relaxes by an emission of a phonon, which has an angular momentum equal to the difference

between the initial and final electron spin.

In conclusion, we have observed spin-coherent transport via discrete energy levels of single Al grains. Spin polarized current saturates quickly as a function of bias voltage, which demonstrates that the ground state and the lowest excited states carry spin polarized current. Higher excited states have a relaxation time shorter than the tunnelling time and they do not carry spin-polarized current. The spin-relaxation time of the low-lying excited states is  $T_1 \approx 0.7 \mu s$  and  $0.1 \mu s$  in two samples, showing that electron spin in a metallic grain is a candidate for quantum information research. Finally, the ratio of the spin-flip transition rate and the electron-phonon relaxation rate is in quantitative agreement with the Elliot-Yafet scaling ratio, an evidence that the spin-relaxation transitions are driven by the spin-orbit interaction.

This work was performed in part at the Georgia-Tech electron microscopy facility. We thank Matthias Braun and Marcus Kindermann for consultation. This research is supported by the DOE grant DE-FG02-06ER46281 and David and Lucile Packard Foundation grant 2000-13874.

---

- [1] D. C. Ralph, C. T. Black, and M. Tinkham, Phys. Rev. Lett. **74**, 3241 (1995).
- [2] O. Agam, N. S. Wingreen, B. L. Altshuler, D. C. Ralph, and M. Tinkham, Phys. Rev. Lett. **78**, 1956 (1997).
- [3] D. Davidović and M. Tinkham, Phys. Rev. Lett. **83**, 1644 (1999).
- [4] J. R. Petta and D. C. Ralph, Phys. Rev. Lett. **87**, 6801 (2001).
- [5] C. T. Black, D. C. Ralph, and M. Tinkham, Phys. Rev. Lett. **76**, 688 (1996).
- [6] M. Johnson and R. H. Silsbee, Phys. Rev. Lett. **55**, 1790 (1985).
- [7] F. J. Jedema, H. B. Heersche, A. T. Filip, J. J. A. Baselmans, and B. J. van Wees, Nature **416**, 713 (2002).
- [8] J. M. Elzerman, R. Hanson, L. H. W. van Beveren, B. Witkamp, L. M. K. Vandersypen, and L. P. Kouwenhoven, Nature **430**, 6998 (2004).
- [9] J. R. Petta, A. C. Johnson, J. M. Taylor, E. A. Laird, A. Y. A. M. D. Lukin, C. M. Marcus, M. P. Hanson, and A. C. Gossard, Science **309**, 2180 (2004).
- [10] D. Loss and D. P. DiVincenzo, Phys. Rev. A **57**, 120 (1998).
- [11] M. Braun, J. Konig, and J. Martinek, Europhys. Lett. **72**, 294 (2005).
- [12] I. Weymann and J. Barnas, Phys. Rev. B **73**, 205309 (2006).
- [13] S. J. van der Molen, N. Tombros, and B. J. van Wees, Phys. Rev. B **73**, 220406 (2006).
- [14] W. Wetzels, G. E. W. Bauer, and M. Grifoni, Phys. Rev. B **74**, 224406 (2006).
- [15] A. Cottet, , and M. S. Choi, Phys. Rev. B **74**, 235316 (2006).
- [16] A. Cottet, T. Kontos, S. Sahoo, H. T. Man, M. S. Choi, W. Belzig, C. Bruder, A. F. Morpurgo, and C. Schonen-

berger, *Semicon. Sci. and Tech.* **21**, S78 (2006).

[17] L. Zhang, C. Wang, Y. Wei, X. Liu, and D. Davidović, *Phys. Rev. B* **72**, 155445 (2005).

[18] A. Bernand-Mantel, P. Seneor, N. Lidgi, M. Munoz, S. F. V. Cros, K. Bouzehouane, C. Deranlot, A. Vauress, F. Petroff, and A. Fert, *Appl. Phys. Lett.* **89**, 062502 (2006).

[19] E. Bonet, M. M. Deshmukh, and D. C. Ralph, *Phys. Rev. B* **65**, 045317 (2002).

[20] S. Adam, M. L. Polianski, X. Waintal, and P. W. Brouwer, *Phys. Rev. B* **66**, 195412 (2002).

[21] Y. Yafet, *Sol. State Phys.* **14**, 1 (1963).

[22] F. J. Jedema, M. S. Nijboer, A. T. Filip, and B. J. van Wees, *Phys. Rev. B* **67**, 085319 (2003).

[23] G. Bergman, *Phys. Rep.* **107**, 1 (1984).